https://doi.org/10.5194/egusphere-2025-3004
Preprint. Discussion started: 9 September 2025

The Dual-Edged Role of Vegetation in Evaluating Landslide Susceptibility: Evidence from Watershed-Scale and Site-Specific Analyses

Songtang He[a, c*], Zhenhong Shen[e], Jeffrey Neal[c], Zongji Yang[a], Jiangang Chen[a], Daojie Wang[a], Yujing Yang[a,b], Peng Zhao[a,b], Xudong Hu[d], Yongming Lin[e], Youtong Rong[c], Yanchen Zheng[f], Xiaoli Su[c], Yong Kong[g]

[a]Key Laboratory of Mountain Hazards and Engineering Resilience, Institute of Mountain Hazards and Environment, Chinese Academy of Sciences, 610213, Chengdu, China

[b]University of Chinese Academy of Sciences, 101408, Beijing, China

[c]School of Geographical Sciences, University of Bristol, BS8 1SS, Bristol, UK

[d]College of Civil Engineering and Architecture, China Three Gorges University, 443002, Yichang, China

[e]College of JunCao Science and Ecology, Fujian Agriculture and Forestry University, China, 350002, Fuzhou, China

[f]School of Civil, Aerospace, and Design Engineering, University of Bristol, BS8 1TR, Bristol, UK

[g]Department of Civil and Environmental Engineering, The Hong Kong Polytechnic University, Kowloon, Hong Kong SAR, China.

[*]Corresponding author. E-mail: hest@imde.ac.cn

Address: No.189, QunXianNan Street, TianFu New Area, Chengdu, Sichuan, China.

https://doi.org/10.5194/egusphere-2025-3004
Preprint. Discussion started: 9 September 2025

Abstract

Vegetation is widely recognized for its beneficial role in landslide mitigation. However, shallow landslides frequently occur even in densely vegetated regions, suggesting that the influence of vegetation on gravity-driven erosion hazards remains incompletely understood. This study investigates the interactive effects of vegetation and key environmental factors—including rainfall, lithology, wind speed, and slope gradient—on landslide susceptibility in an area with substantial vegetation cover (≥65.5%). At the watershed scale, we employed structural equation modeling and geographic detectors to assess the primary drivers of landslide susceptibility under high vegetation conditions. At the point scale, we calculated the stability coefficient of a representative landslide, accounting for both vegetation self-weight and artificial waste sediment. Our findings reveal that the combination of vegetation, rainfall, and wind speed significantly increases landslide susceptibility, as evidenced by a 21.3% rise in high and very high susceptibility zones and a 42.7% reduction in low and very low susceptibility zones. Interactions among multiple factors exerted a stronger influence than individual factors, with the most pronounced interaction observed between slope gradient and rainfall (Geodetector q = 0.81), followed by rainfall and lithology (q = 0.79). Under saturated conditions, the stabilizing effect of root systems was outweighed by the self-weight of tree vegetation, leading to a marked decrease in slope stability compared to scenarios without additional loading. These results offer new insights into the complex role of vegetation in landslide control and highlight the importance of considering interactive environmental effects at multiple spatial scales.

https://doi.org/10.5194/egusphere-2025-3004
Preprint. Discussion started: 9 September 2025

Keywords: shallow landslide; high vegetation mountainous area; landslide susceptibility; structural equation model; vegetation self-weight

https://doi.org/10.5194/egusphere-2025-3004
Preprint. Discussion started: 9 September 2025

1 Introduction

The prevalence of landslide hazards in regions with high vegetation cover suggests complex mechanisms in the relationship between vegetation and landslides (He et al., 2017; Xu et al., 2024), which extend beyond a linear association (Lan et al., 2020). Therefore, more research is needed to understand how slope stability and environmental factors interact under good vegetation cover conditions (Cui et al., 2024; Deng et al., 2022; Medina et al., 2021). Accurate hazard assessment and mitigation depend on understanding the interactions between vegetation, slope morphology, and landslide occurrence (Alvioli et al., 2024; Zhang et al., 2025)

Vegetation cover inhibits soil erosion, regulates soil moisture, and stabilizes slopes via root networks that anchor the soil (He et al., 2017), and ultimately improves slope morphology and soil structure to stabilize the slope. Therefore, higher vegetation cover is generally believed to help prevent landslide hazards (Rey et al., 2019). However, a recent work reposted that vegetation can reduce gully erosion but promote shallow landslides (Xu et al., 2024). Thus, vegetation can also increase landslide susceptibility by adding weight and altering soil properties (Qin et al., 2024). For example, trees represent a balance between root reinforcement and the destabilizing effect of tree weight, influenced by slope gradient (Schmaltz & Mergili, 2018). Additionally, wind forces can destabilize steep slopes (Bordoloi & Ng, 2020). On thin-soil slopes, root wedging may cause fractures, increasing susceptibility to external disturbances (Liu et al., 2020). Rainfall, a major trigger of landslides (Dhanai et al., 2022), saturates soil on slopes, reducing soil cohesion and shear resistance. When the shear strength is

https://doi.org/10.5194/egusphere-2025-3004
Preprint. Discussion started: 9 September 2025

insufficient to counteract the downslope forces generated by gravitational water distribution, instability occurs, amplifying the destructive effects (Li et al., 2025). Areas with high vegetation cover typically have favorable moisture and temperature conditions. Although vegetation roots play an effective role in stabilizing soil, vegetation can also alter soil properties by increasing soil moisture content or reducing soil density, which affects matrix cohesion (Gonzalez-Ollauri & Mickovski, 2016; Murgia et al., 2022; Vergani et al., 2017). Therefore, in areas with high vegetation cover, the occurrence of landslide hazards is influenced by multiple spatial factors, such as soil texture, vegetation, and rainfall. Investigating which factors primarily drive the initiation (Xu et al., 2024), and how the combined effects of these factors influence the occurrence and development of landslides, has become a key issue in landslide forecasting and risk zoning. Consequently, further study of the relationship between vegetation with environmental factors, and landslide is of significant importance.

Early studies used geoscience factor weights, logistic models, and Geographic Information Systems (GIS) spatial analysis to assess the environmental factors that are responsible for landslides (Regmi et al., 2010; Yilmaz, 2009). While these revealed spatial distribution patterns, they focused on qualitative descriptions and analyses and rarely addressed spatial correlations or interactions between factors. Few studies have thoroughly explored the spatial correlation of factors contributing to landslides and debris flows, resulting in a lack of quantitative representation of spatial correlations in disaster risk. Research on vegetation types, height, and growth conditions (such as slope and human disturbances) in relation to landslide risks remains limited. While,

https://doi.org/10.5194/egusphere-2025-3004
Preprint. Discussion started: 9 September 2025

significant progress has been made on the relationship between rainfall and landslides (Ortiz-Giraldo et al., 2023), using models based on spatial autocorrelation (for example, Moran's I and Geary's C indices) and clustering methods (Chen et al., 2024; Liu et al., 2024; Pokharel et al., 2021; Schmaltz & Mergili, 2018; Wang et al., 2020), the mechanisms of interaction between these factors remain unclear particularly the modifying influence of vegetation on slope stability coefficients (Lan et al., 2020). Overall, the dynamic processes through which vegetation and environmental factors interact to shape landslide occurrences are still not well understood. To clarify how rainfall, slope, lithology, and soil thickness influence landslides in well-vegetated areas—and to explore vegetation's "double-edged sword" role in landslide mitigation—this study examines the relationship between environmental factors and landslide occurrence by integrating watershed-scale analysis with point-scale mechanistic insights. In summary, focusing on the frequent occurrence of landslides and debris flows in areas with high vegetation cover, this study selects a vegetation-rich region in Southwest China as the study area. Through field investigations and remote sensing image analysis, the study employs the Geodetector method and structural equation modeling to analyze the influencing factors and mechanisms of landslide susceptibility under a high-vegetation background at a macroscopic scale. Meanwhile, at the microscopic level, it examines the role of vegetation as a mediator in coupling with other factors (wind force, slope gradient, and load) in typical landslide occurrences within the region. By integrating watershed scale and typical point landslide analyses for mutual verification and interpretation, this study lays the foundation for elucidating

https://doi.org/10.5194/egusphere-2025-3004
Preprint. Discussion started: 9 September 2025

the dual role of vegetation in landslide prevention and mitigation.

2 Methods and materials

2.1 Study area

The study area is in Jinkouhe District, Sichuan Province, China (102°50′24″–103°10′24″ E, 29°00′24″–29°00′46″ N). The Dadu River flows in a north-south "S" shape through the 598 km² region, which is 99% mountainous, with complex geological structures. Rock types include slate, clastic rocks, dolomite, limestone, and basalt. Forest coverage is 65.55%, and the terrain slopes from southwest to northeast with elevations ranging from 530 to 3,321 m, and a vertical drop of 2,700 m (**Fig. 1**). Jinkouhe District has a subtropical monsoon climate with a warm and humid atmosphere, abundant sunshine, and distinct seasons. The annual average temperature is 15°C, with highs of 38°C and lows of -9°C. Precipitation averages 1252.6 mm annually, concentrated in the summer, while average annual evaporation is 677.3 mm with dry winters, spring droughts, frequent summer floods, and prolonged autumn rainfall.

https://doi.org/10.5194/egusphere-2025-3004
Preprint. Discussion started: 9 September 2025

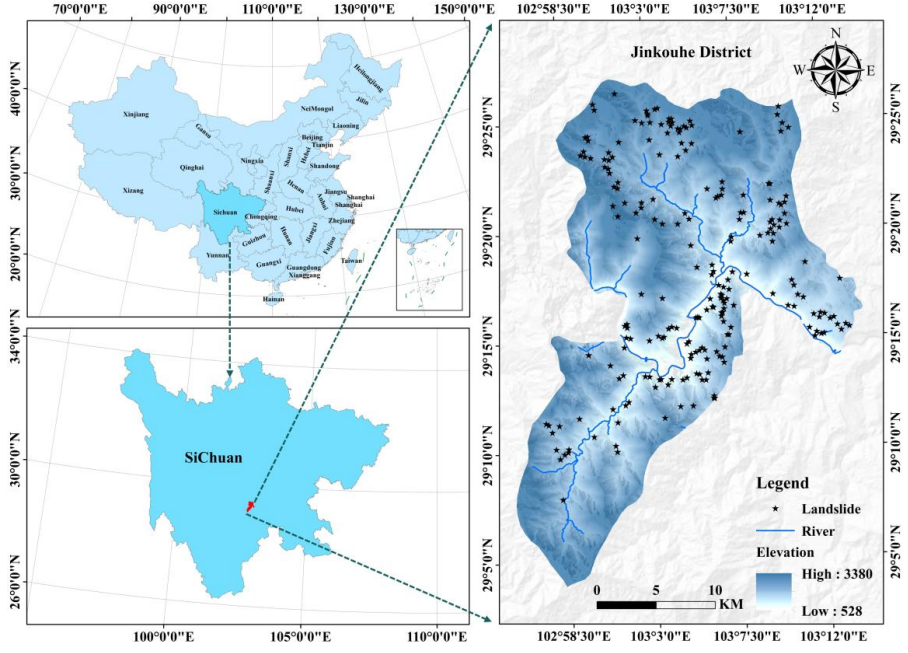

Fig. 1. Location map of Jinkouhe District

A major landslide occurred in the study area on June 4, 2023, near the living quarters of a Phosphate Mine (103°2′25.75″ E and 29°25′0.6″ N). According to the 2021 geological disaster risk assessment report for the Jinkouhe District, the collapse site is located within a high geological disaster susceptibility and medium-risk zone. The disaster was preceded by continuous rainfall.

https://doi.org/10.5194/egusphere-2025-3004
Preprint. Discussion started: 9 September 2025

Fig. 2. Schematic of Satellite Image Before Landslide Occurrence (basic picture from © Google Earth)

In front of the collapsed area were the mine's living quarters. To the left, 70 m away, was the entrance to Tunnel No. 2, and 15 m behind it was a water diversion tunnel entrance (**Fig. 2**). During the construction of the diversion tunnel, 400 m^3 of waste rock was deposited, adding approximately 800 tons of load, bringing the slope in the instability initiation zone to a critically stable state. The disaster was preceded by continuous rainfall. On May 31, 2023, moderate to heavy rainfall in the Jinkouhe area caused surface overland flow in a 0.1 km^2 catchment area at the top of the gully Vegetation increased water storage, and surface runoff infiltrated the Cambrian lower formation dolomitic limestone, generating significant groundwater. This groundwater flowed down along fractures and bedding planes but was obstructed by the sandstone and shale aquitard raising the groundwater level. Saturation of gravelly clay at the basal

https://doi.org/10.5194/egusphere-2025-3004
Preprint. Discussion started: 9 September 2025

interface softened the soil, reducing its shear strength and forming a slip surface, triggering landslide. The shape of the landslide was elongated, resembling a "tongue." The elevation ranged from 2,303 m at the rear to 2,183 m at the front, a height difference of 120 m. The slope was 308 m long, and the collapse width ranged from 18 m to 41 m, averaging 36 m. The maximum height of the rear scarp was 12 m. The collapse created a residual body and deposition area, covering a total area of 10,186 m². The collapse direction was 80°, with scouring in the center lateral deposits forming at the front edge (**Fig. 3**).

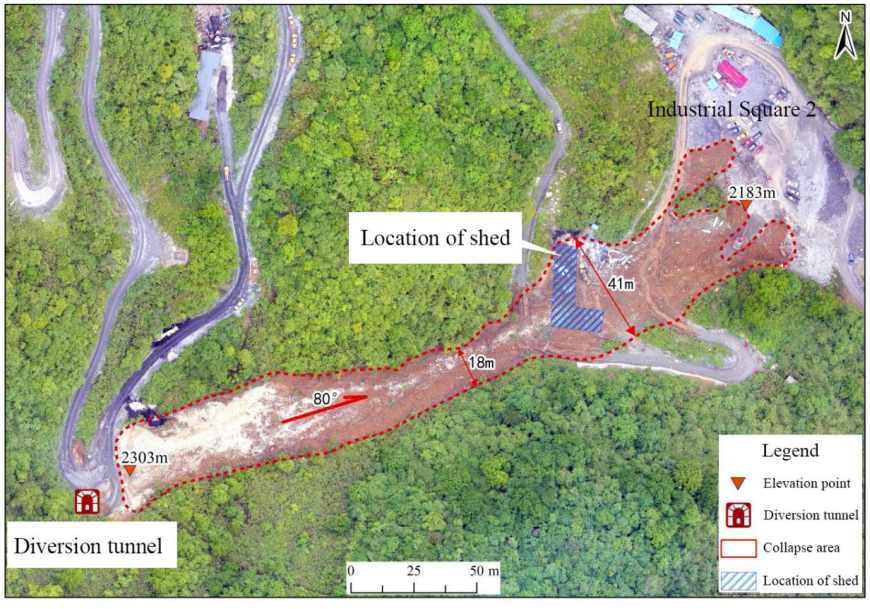

Fig. 3. Schematic of the UAV image after the landslide

2.2 Data source and preprocessing

The following data are required for landslide susceptibility analysis and spatial correlation of triggering factors in the study area.

https://doi.org/10.5194/egusphere-2025-3004
Preprint. Discussion started: 9 September 2025

(1) **ASTER GDEM Digital Elevation Model** data with a resolution of 30 m were obtained from a Geospatial Data Cloud (https://www.gscloud.cn/). Slope and aspect factor data were extracted using surface analysis.

(2) **Road and river vector files** were obtained from Open Street Map (https://www.openstreetmap.org/).

(3) **Lithology data** (Hengl et al., 2017) with a resolution of 250 m were acquired from NASA's Open Data Center (https://search.earthdata.nasa.gov/).

(4) **Fault data** were obtained from the National Earthquake Science Data Center (https://data.earthquake.cn/).

(6) **Maximum NDVI raster data** for China in 2021 with a resolution of 30 m and 2021 wind speed data with a resolution of 1 km (Xu, 2022a, 2022b) were obtained from the Resource and Environment Science and Data Center of the Chinese Academy of Sciences (https://www.resdc.cn/).

(7) **Monthly rainfall raster data** from 2018 to 2023 with a resolution of 1 km (Peng, 2024), obtained from the National Tibetan Plateau Data Center (https://data.tpdc.ac.cn/). To eliminate the random effects of precipitation, the multi-year average annual precipitation was used as the influencing factor. Annual precipitation was first calculated using map algebra, and then the multiyear average annual precipitation was derived.

(8) **Landslide hazard point data** were obtained from the GeoCloud platform (https://geocloud.cgs.gov.cn/). Additionally, 227 landslide points were identified through the manual interpretation of remote sensing images.

https://doi.org/10.5194/egusphere-2025-3004
Preprint. Discussion started: 9 September 2025

All datasets were unified to the WGS_1984_UTM_Zone_47N coordinate system and the pixel size was standardized to 30 m × 30 m. The processed results are shown in Fig. S1.

2.3 Landslide susceptibility evaluation framework

2.3.1 landslide susceptibility based on the analytic hierarchy process (AHP)

Landslide susceptibility analysis was conducted by overlaying landslide sites with elevation, slope, aspect, distances to faults, rivers, roads, lithology, rainfall, Normalized Difference Vegetation Index (NDVI), and wind speed. All factors passed the multicollinearity test with variance inflation factor (VIF) values below 10 (Arabameri et al., 2019; Chen et al., 2018). Range normalization was applied to standardize all indicators (He et al., 2024). A comprehensive multi-factor evaluation combined weight calculations and GIS-based methods, including buffer, statistical, and overlay analysis. Factors were classified and assigned weights, and validated using consistency tests (Table S1). The overlay analysis produced a landslide susceptibility distribution map of the study area (Ahmad et al., 2023; Asmare, 2023), with susceptibility categorized into five levels: very low, low, medium, high, and very high, based on existing standards.

The landslide susceptibility index (SI) is calculated as:

$$SI = \sum w_i IF_I \quad (1)$$

where SI is the comprehensive geological hazard susceptibility index for the evaluation unit; w_i represents the weight of the influencing factor; and IF_i represents the value of the influencing factor.

The process involved altering the influencing factors to examine how

https://doi.org/10.5194/egusphere-2025-3004
Preprint. Discussion started: 9 September 2025

environmental variables (rainfall, vegetation, and wind speed) affect landslide susceptibility. Common factors included elevation, slope, aspect, lithology, and distances to faults, rivers, and roads. Vegetation, rainfall, and wind speed were added successively, resulting in five scenarios.

Class I: Common factors.

Class II: Common factors + vegetation.

Class III: Common factors + rainfall.

Class IV: Common factors + vegetation + rainfall.

Class V: Common factors + vegetation + rainfall + wind speed.

The consistency ratio (*CI*) values for the five scenarios were 0.07, 0.09, 0.07, 0.08, and 0.07, respectively, all of which were < 0.1, indicating that they passed the consistency test (Table S2). Table S3 presents the eigenvectors and weights. The formulas for calculating the Consistency Index and Consistency Ratio are as follows:

$$CI = \frac{\lambda_{max} - n}{n - 1} \quad (2)$$

$$CR = \frac{CI}{RI} \quad (3)$$

Where: RI is the random index (from the lookup table); λ_{max} is the maximum eigenvalue, and n is the number of factors.

2.3.2 Rationality validation of susceptibility assessment results

In this study, Receiver Operating Characteristic (ROC) curves and area under the curve (AUC) values were used for validation. ROC curves provide a representation of the specificity and sensitivity of an analytical method (Khosravi et al., 2019; Yilmaz, 2009). The AUC measures model accuracy, ranging from 0.5 to 1, with values closer to

https://doi.org/10.5194/egusphere-2025-3004
Preprint. Discussion started: 9 September 2025

1 indicating higher accuracy (Sezer et al., 2010).

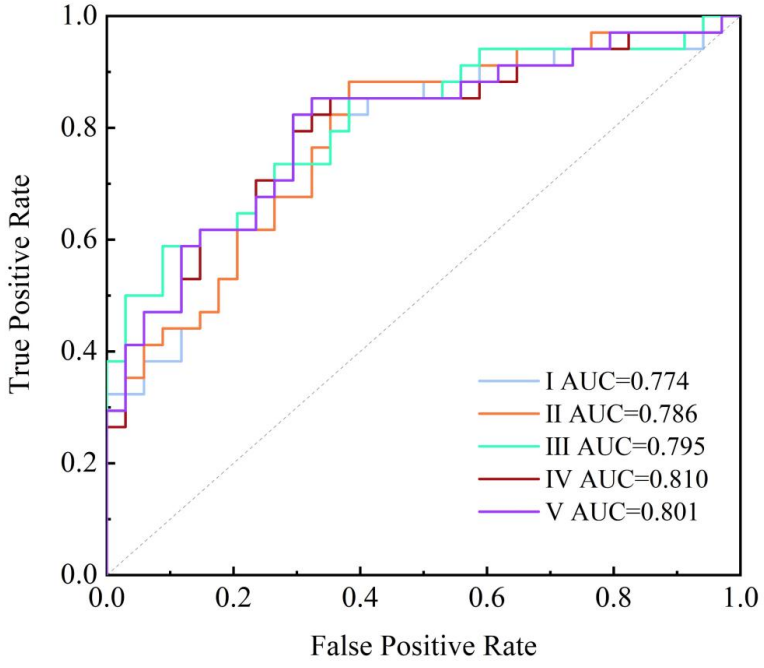

Fig. 4. ROC curve of geological hazard susceptibility assessment results

Based on the susceptibility distribution map, landslide point data obtained from the Geological Cloud platform were selected, and an equal number of non-landslide points were created to plot the ROC curve for landslide susceptibility. AUC values for the five scenarios were 0.774, 0.786, 0.795, 0.81, and 0.801, respectively, all exceeding 0.5, indicating good accuracy in the landslide susceptibility evaluation (**Fig. 4**).

2.4 Landslide driving mechanism analysis based on GeoDetector and structural equation model

The occurrence of landslides is associated with numerous factors. To identify the dominant ones influencing landslide susceptibility, the GeoDetector method was applied. This method examines the spatial differentiation of individual variables and

https://doi.org/10.5194/egusphere-2025-3004
Preprint. Discussion started: 9 September 2025

the interaction effects of two factors on the dependent variable, revealing their explanatory power regarding landslide susceptibility. Furthermore, a structural equation model (SEM), with its ability to analyze complex relationships among variables, was employed to reveal how various factors interact to trigger landslides. (See **Fig. 5**).

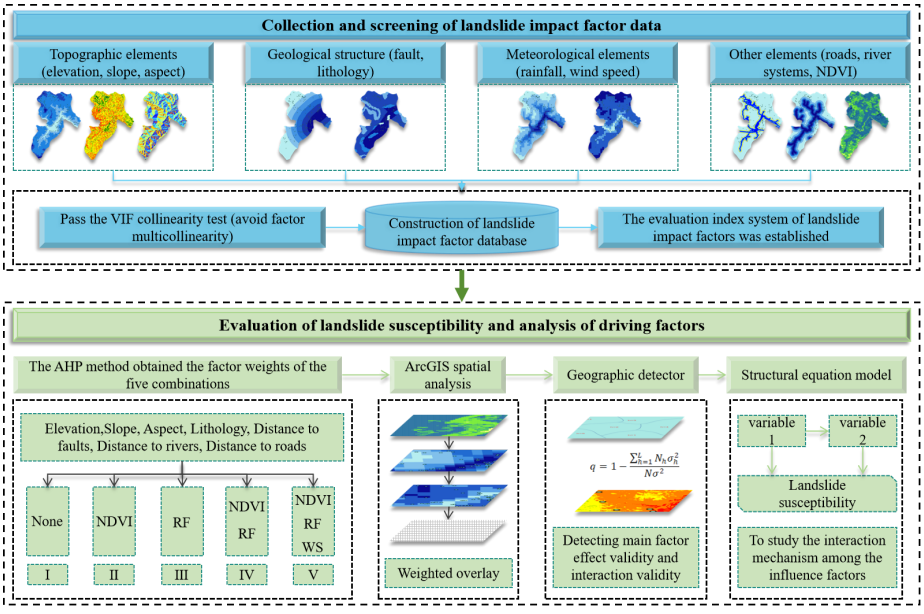

Fig. 5. Technical Workflow Diagram

(1) GeoDetector

Geo detection identifies spatially stratified variations and patterns of geographic phenomena, addressing spatial dependence and heterogeneity caused by scale changes that traditional statistical methods cannot resolve (Ng et al., 2021; Wang et al., 2010). This study applied factor and differentiation to explore drivers of landslide susceptibility in high vegetation areas. In single-factor detection, landslide susceptibility was the dependent variable, and each evaluation factor was used as an explanatory variable to identify key drivers influencing geological hazard risk (Lu et

https://doi.org/10.5194/egusphere-2025-3004
Preprint. Discussion started: 9 September 2025

al., 2024; Yang et al., 2024). Interaction detection evaluated whether the combined effect of two factors increased or reduced explanatory power compared to their individual effects, revealing interactions between variables. The influence of factors is quantified by the *q*-value (0 to 1), with values closer to 1 indicating stronger spatial differentiation explanatory power. The formula is:

$$q = 1 - \frac{\sum_{h=1}^{L} N_h \sigma_h^2}{N\sigma^2} \quad (4)$$

where h denotes the number of classifications or partitions for a specific indicator. L represents the stratification of variable Y or factor X (i.e., classification or partitioning). N is the total number of units in the study area. N_h is the number of units in the *h-th* stratum. σ^2 and σ_h^2 are the variances of landslide susceptibility in the entire study area and the *h-th* stratum, respectively.

(2) Structural equation model

The SEM comprises two components: the measurement model, which defines relationships between observed and latent variables, and the structural model, which illustrates relationships among latent variables (Fan et al., 2016; Wang & Rhemtulla, 2021). Using GeoDetector results, SEM was used to analyze interactions among key factors influencing landslide susceptibility. Based on literature and micro-mechanisms (Chicas et al., 2024; Pourghasemi et al., 2018; Segoni et al., 2024), the following hypotheses were proposed:

- Slope, lithology, distance to fault, distance to road, distance to river, rainfall, and vegetation directly affect landslide occurrence
- Elevation and faults indirectly affect landslides by influencing vegetation

https://doi.org/10.5194/egusphere-2025-3004
Preprint. Discussion started: 9 September 2025

types and distribution

- Wind speed and river impact vegetation growth
- Rivers and elevation influence rainfall through the water vapour cycle
- Vegetation and wind speed indirectly influence landslide susceptibility by influencing rainfall infiltration and local rainfall variations.

The SEM was constructed using RStudio software, and the path coefficients and parameters were estimated using the maximum likelihood method.

Measurement model:

$$X = \Lambda_x \xi + \varepsilon_1 \quad (5)$$

$$Y = \Lambda_y \xi + \varepsilon_2 \quad (6)$$

Structural model:

$$\eta = B \times \eta + \Gamma \times \xi + \varepsilon_3 \quad (7)$$

where X/Y is the vector of exogenous/endogenous indicators. Λx / Λy is the factor loading matrix of exogenous indicators for exogenous/endogenous latent variables. ξ represents the exogenous latent variables. η represents endogenous latent variables. B represents the relationships among endogenous latent variables, Γ indicates the effect of exogenous latent variables on endogenous latent variables. ε_1、ε_2、ε_3 are the error terms for exogenous indicators, endogenous indicators. The residual term represents the unexplained portion of the endogenous latent variables within the equation. The final model fit results are summarized in Table S4 (Hu & Bentler, 1999; Stone, 2021).

2.5 Landslide stability calculation considering vegetation weight

Based on the field survey, constructing the drainage tunnel added an additional 400 m³ of waste material, with a weight of approximately 800 tons, along with 500 trees,

https://doi.org/10.5194/egusphere-2025-3004
Preprint. Discussion started: 9 September 2025

each with an average weight of 60 kg. The collapsed mass was composed of gravel-clay with a high moisture content, exhibiting a plastic state. The slopes natural unit weight was γ = 19.5 kN/m^3, and the saturated unit weight was γ_w = 20 kN/m^3. The natural shear strength was c = 15.5 kPa, with an internal friction angle of 10.5°, and the saturated shear strength was c = 15.0 kPa, with the same friction angle. The slope stability was calculated using the formula for tree-vegetated slopes from Lan et al. (2022), accounting for the effects of artificial waste material and vegetation weight. The formula is:

$$F_s = \frac{\sum(c_i l_i + G_i \cos\theta_i \tan\varphi_i + F_i)}{\sum(G_i + G_i')\sin\theta_I} \quad (8)$$

where: F_i represents the anchoring force of the vegetation's vertical roots; G_i' denotes the downward gravitational force exerted by the vegetation; Gi refers to the vertical gravitational force acting on the soil mass; i represents the length of the sliding arc, φ_i is the internal friction angle, and θ_i is the angle between the i-th sliding block and the vertical direction. The stress analysis of the slope, incorporating the weight of the vegetation, is illustrated in Fig. 6.

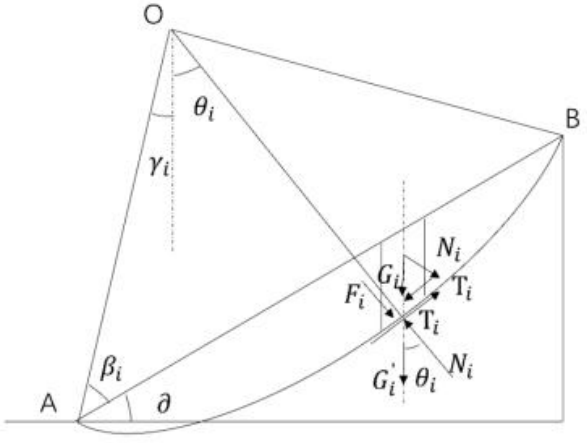

https://doi.org/10.5194/egusphere-2025-3004
Preprint. Discussion started: 9 September 2025

318 **Fig. 6. Slope Stress Analysis Diagram**

319 # 3 Results

320 ## 3.1 Landslide susceptibility mapping and distribution characteristics

321 Fig. 7 and Table 1 present the landslide susceptibility results considering
322 environmental factors (rainfall, vegetation, and wind speed) along with common factors
323 (elevation, slope, aspect, lithology, distance to fault, river, and road). Most of the study
324 area shows moderate landslide susceptibility, with 84 landslides covering 53.77% of
325 the total area. Low and very low susceptibility zones contained 30 landslides covering
326 16% of the area. High and very high susceptibility zones, occupying 30.23% of the
327 study area, experienced 113 landslides.

328 Moderate susceptibility zones are widespread across the northern, western, and
329 southwestern regions. High and very high susceptibility zones, though smaller in
330 coverage, are primarily located in the central-eastern region. High susceptibility zones
331 display a "cross-shaped" spatial distribution, while very high susceptibility zones are
332 scattered within the high susceptibility areas.

333 **Table 1. Distribution of landslide susceptibility zones in Jinkouhe District**

Susceptibility Zone	Number of Landslides (count)	Zoning Area (km^2)	Proportion of landslide points in the total (%)	Proportion of zone to total area (%)	Landslide Point Density (points/km^2)
Very low	1	7.33	0.44	1.21	0.14
Low	29	89.43	12.78	14.79	0.32
Mid	84	325.06	37.00	53.77	0.26
High	105	167.26	46.26	27.67	0.63
Very high	8	15.49	3.52	2.56	0.52

https://doi.org/10.5194/egusphere-2025-3004
Preprint. Discussion started: 9 September 2025

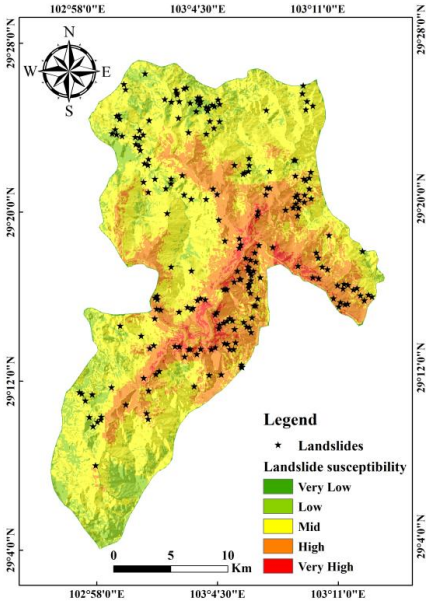

Fig. 7.Landslide susceptibility assessment map

3.2 Relationship between H/L and area of a typical landslide

Landslide parameters for each segment, including height, travel distance, and landslide area (Table S5), along with overall landslide parameters (**Table 2**), were measured. The total landslide height (H) is 120 m, with an average collapse width of 36 m. Travel distances increase sequentially across the three segments, with the deposition zone having the longest at 110.9 m. The total landslide travel distance (L), calculated as the sum of all segments, is 283.3 m.

Table 2. Main morphological parameters of landslide

Data types	Number
Total landslide area (m^2)	1×10^4
Total landslide volume (m^3)	3.1×10^4
Total landslide length (m)	308
Landslide starting point elevation (m)	2303
Landslide endpoint elevation (m)	2183
Landslide height (m)	120
Landslide movement distance (m)	283.3
H/L	0.42

https://doi.org/10.5194/egusphere-2025-3004
Preprint. Discussion started: 9 September 2025

As travel distance increases, the landslide area expands rapidly from the initial instability zone (2147 m²), scraping away surrounding soil, and eventually forming a deposition area of 5234 m². The final total landslide area was10,000 m².

Using the landslide height (H) and maximum travel distance (L), H/L was calculated to be 0.42, which was less than 0.60, classifying it as a general or medium-sized landslide. Although its activity intensity and destructive potential may be lower than those of high-speed, long-runout landslides, its potential hazard level remains moderate to relatively high (Text S1).

3.3 Evaluation results of slope stability considering artificial waste sediment and vegetation self-weight

Table 3 shows stability results under four conditions: natural and saturated states without and with the loading of artificial waste sediment and vegetation self-weight. Results indicate that the slope remained stable under natural and saturated conditions without loading, with greater stability in the natural state. Under natural conditions with waste sediment loading, the slope was stable. However, under saturated conditions, with both waste and vegetation self-weight loadings, the slope became unstable and failed. Comparing results revealed that the self-weight of materials in the natural state was even greater than those in the saturated state.

Table 3. Stability results under different conditions

Geotechnical condition	Without waste material and vegetation		With waste material and vegetation	
	Natural Condition	Water-saturated	Natural Condition	Water-saturated
Stability Factor (Fs)	1.21	1.13	1.02	0.89

https://doi.org/10.5194/egusphere-2025-3004
Preprint. Discussion started: 9 September 2025

4 Discussion

4.1 Analysis of landslide driving forces and mechanisms

Based on the distribution of landslide occurrences within different thresholds of the influencing factors (Text S2), landslides in areas with good vegetation conditions are controlled by multiple factors. **Table 4** shows the explanatory power of each factor for landslide susceptibility, ranked as follows: rainfall > elevation > distance to fault > distance to river > wind speed > lithology > slope > distance to road > NDVI.

Table 4. Explanatory power of each factor on landslide susceptibility

	X1	X2	X3	X4	X5	X6	X7	X8	X9	X10
q statistic	0.55	0.28	0.06	0.40	0.49	0.28	0.46	0.27	0.63	0.44
rank	2	7	10	6	3	8	4	9	1	5

Note: X1–X10 represent elevation, slope, aspect, lithology, distance to fault, distance to road, distance to river, NDVI, rainfall, and wind speed, respectively.

Further analysis using interaction detection assessed the explanatory power of interactions between factors for landslide susceptibility (**Fig. 8**). Among 45 pairs of interacting factors, 40 exhibited bifactor enhancement, and five pairs showed nonlinear enhancement, with no independence or weakening observed. Bifactor interactions had a significantly stronger influence on landslide susceptibility than single factors. The most impactful interaction was between slope and rainfall (q=0.81), followed by rainfall and lithology (q=0.79). Rainfall interactions with other factors exceeded 70%, and fault distance interactions surpassed 60%. Wind speed interactions with elevation, slope, rainfall, lithology, distance to road, and NDVI exhibited bifactor enhancement all above 50%. Similarly, NDVI interactions with elevation, rainfall, lithology, distance to fault, road, and river, and wind speed also showed bifactor enhancement, with influence levels exceeding 50%. From the results of the factor interactions, the

https://doi.org/10.5194/egusphere-2025-3004
Preprint. Discussion started: 9 September 2025

synergistic effects of rainfall, fault distance, lithology, NDVI, and wind speed emerged as the dominant interaction modes driving landslide susceptibility.

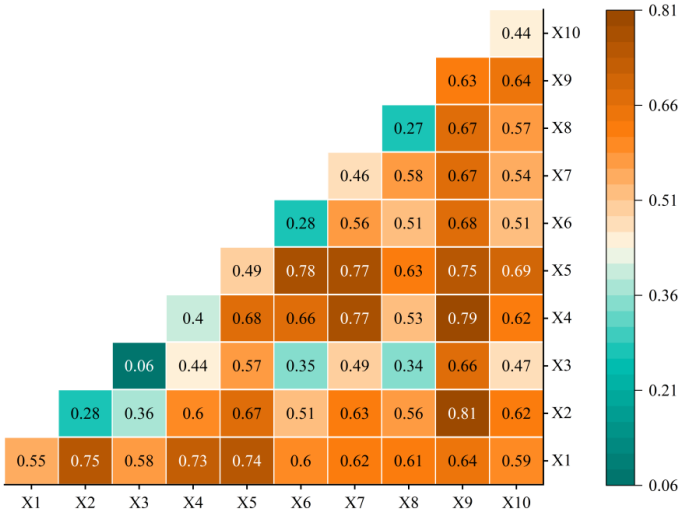

Fig. 8. Explanatory Power of Interactions Between Factors on Landslide Susceptibility.

Note:X1–X10 represent elevation, slope, aspect, lithology, distance to fault, distance to road, distance to river, NDVI, rainfall, and wind speed, respectively.

To further clarify how various factors interact and contribute to landslide occurrence, an SEM was constructed (Table S4) using the key factors identified by the GeoDetector (excluding aspect). The SEM explained 92% of the landslide susceptibility variance, with all factors showing significant correlations ($p < 0.01$) (**Fig. 9**, **Table 5**). The influence of each showed varying direct and indirect effects. Slope had the greatest impact, with a total effect coefficient of 0.33, attributed to direct effects (coefficient: 0.33). Steeper slopes increased the likelihood of landslides. The total effect coefficient of distance to fault (0.30) was second only to slope, primarily reflected as a direct effect (0.27), with a minimal indirect effect coefficient of 0.03. This is because faults occur where the structural stability of the slopes is poor. Fault zones can cause

https://doi.org/10.5194/egusphere-2025-3004
Preprint. Discussion started: 9 September 2025

localized stress and weaken the structural integrity of slopes. This is particularly true in the study area, which lies at the intersection of the Longquanshan Fault Zone and the Ebian-Mabian Seismic Belt located in the central segment of China's north–south seismic belt. Proximity to faults increases the susceptibility of rock and soil structures to fault ruptures, thereby raising landslide susceptibility. Faults also allow water infiltration, altering soil moisture and groundwater levels, and thereby influencing landslide-triggering conditions. For instance, increased rainfall may elevate pore water pressure in the soil and release through fault zone weak points, further heightening landslide susceptibility.

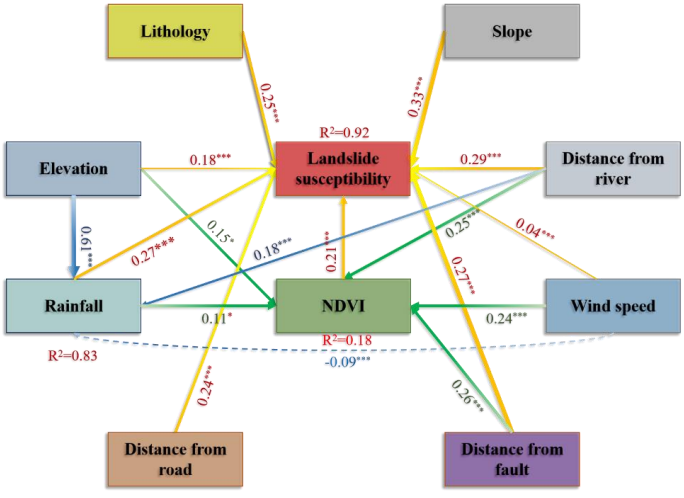

Fig. 9. SEM of landslide susceptibility.

Note: Rectangles = observed variables; unidirectional arrows = relationship between two variables. The variable at the arrowhead is influenced by the variable at the arrow's base. The numbers near the yellow single arrows represent the total effect coefficients of factors on landslide susceptibility. Arrows in other colors indicate the standardized normalized influence coefficients between factors. Solid arrows = positive = relationships; R^2 = proportion of variance explained. ***, **, and * denote significance levels of 0.01, 0.05, and 0.1, respectively.

The total effect coefficient of the distance to the river was 0.29, primarily reflected

https://doi.org/10.5194/egusphere-2025-3004
Preprint. Discussion started: 9 September 2025

as a direct effect (coefficient: 0.2). The indirect effect (coefficient: 0.09) mainly influences landslides indirectly through NDVI and rainfall. The total effect coefficient of rainfall on landslides is 0.27, with a direct effect coefficient of 0.24. This is primarily because rainfall increases soil moisture content and bulk density while reducing soil shear strength. As soil moisture continues to accumulate, transient additional water loads form, further weakening slope stability. Rainfall also generates surface runoff, eroding slopes, damaging the slope structure, and thus increasing landslide susceptibility. Its indirect effect (coefficient: 0.03), comes from groundwater recharge and altered water flow paths modifying slope morphology over time and heightening landslide risk.

Table 5. Influence of various factors on landslide susceptibility

Factor	Total effect	Direct effect	Indirect effect
Elevation	0.18	0	0.18
Slope	0.33	0.33	0
Lithology	0.25	0.25	0
Distance from fault	0.30	0.27	0.03
Distance from road	0.24	0.24	0
Distance from river	0.29	0.2	0.09
NDVI	0.21	0	0.21
Rainfall	0.27	0.24	0.03
Wind speed	0.04	0	0.04

In terms of direct effects, lithology has a total effect coefficient of 0.25 on landslides, entirely direct. Lithology provides the material basis for landslides as soil layers formed by different lithologies vary in shear strength and permeability. In the study area, soft rocks, such as shale and clastic rocks, which became loose and highly weathered after absorbing water, exhibited strong deformation and a high likelihood of causing landslides. Roads had a total effect coefficient of 0.24, which was also entirely

https://doi.org/10.5194/egusphere-2025-3004
Preprint. Discussion started: 9 September 2025

direct. This is because road construction often involves slope excavation and vegetation destruction, directly altering the stability of the natural terrain. Poorly designed road drainage can also cause water to accumulate, affecting slope stability over time.

Regarding indirect effects, wind speed has an influence coefficient of only 0.04. Generally, wind alone cannot directly destabilize a slope, but affects stability through drag forces. Strong winds can strip soil cover, accelerating moisture evaporation, leading to surface cracks and reducing structural stability. Higher elevations (effect: 0.18) imply more rainfall and weathering, but are not direct landside triggers. NDVI had a total effect coefficient of 0.21 indirectly enhancing slope stability. through vegetation roots which improve soil cohesion and shear strength. However, root systems can cause deformation, increasing water infiltration and reducing slope stability. This effect can be particularly pronounced in areas with dense, well-developed root systems. Tall trees on steep slopes can reduce stability due to weight and wind drag. Vegetation also indirectly regulates soil moisture through transpiration, reducing pore water pressure, which affects slope stability.

In summary, vegetation mediates multiple factors, amplifying their combined effects on landslide susceptibility. Interactions between vegetation and other factors are crucial in assessing landslide risks.

4.2 Comparison of landslide susceptibility results under different influence factor combinations

It has been demonstrated that vegetation, wind, and rainfall have varying direct or indirect impacts on landslide susceptibility. These impacts are based on the statistical

https://doi.org/10.5194/egusphere-2025-3004
Preprint. Discussion started: 9 September 2025

relationship between thresholds of influencing factors and the number of landslides, as well as the contributions of various factors to landslide susceptibility through direct or indirect effects analyzed using GeoDetector and SEM. The spatial distribution and statistical data of landslide susceptibility under the influence of various environmental factors (rainfall, vegetation, and wind) are depicted in **Fig. 10** and **Table 6**: taking into account public factors alone (Category I), public factors + vegetation (Category II), public factors + rainfall (Category III), public factors + vegetation + rainfall (Category IV), and public factors + vegetation + rainfall + wind (Category V).

Table 6. Distribution of landslide susceptibility zones for the five scenarios

	I		II		III		IV		V	
	Area	Quantity	Area	Quantity	Area	Quantity	Area	Quantity	Area	Quantity
Very low	15.63	7	13.68	2	7.74	1	8.79	1	7.33	1
Low	150.19	43	155.30	50	100.09	24	123.91	39	89.43	29
Mid	284.81	87	291.75	87	313.12	97	303.06	80	325.06	84
High	128.85	78	133.11	83	150.40	85	152.51	97	167.26	105
Very high	25.08	12	10.72	5	33.21	20	16.30	10	15.49	8
Total	604.56	227	604.56	227	604.56	227	604.56	227	604.56	227

The results indicate that using Category I as the baseline, adding vegetation independently (Category II) decreases very low and very high susceptibility zones by 14.37 km² and 1.95 km², respectively, with fewer landslides. Other zones saw slight increases, with the low susceptibility zone increasing by 15.11 km² and seven additional landslides, suggesting that vegetation inhibits landslides.

When rainfall is added independently (Category III), overall susceptibility increases significantly. Very low and low susceptibility zones decrease by a total of

https://doi.org/10.5194/egusphere-2025-3004
Preprint. Discussion started: 9 September 2025

57.99 km², and the medium susceptibility zones increase by 28.31 km² with 10 additional landslides. The high and very high susceptibility zones increase by 29.69 km² with 15 additional landslides. This indicates that vegetation has a positive inhibitory effect on landslide occurrences in favorable eco-geological conditions (such as terrain, slope, and altitude). However, in high or very high susceptibility zones with harsh conditions, rainfall amplifies vegetation's contribution to landslide susceptibility.

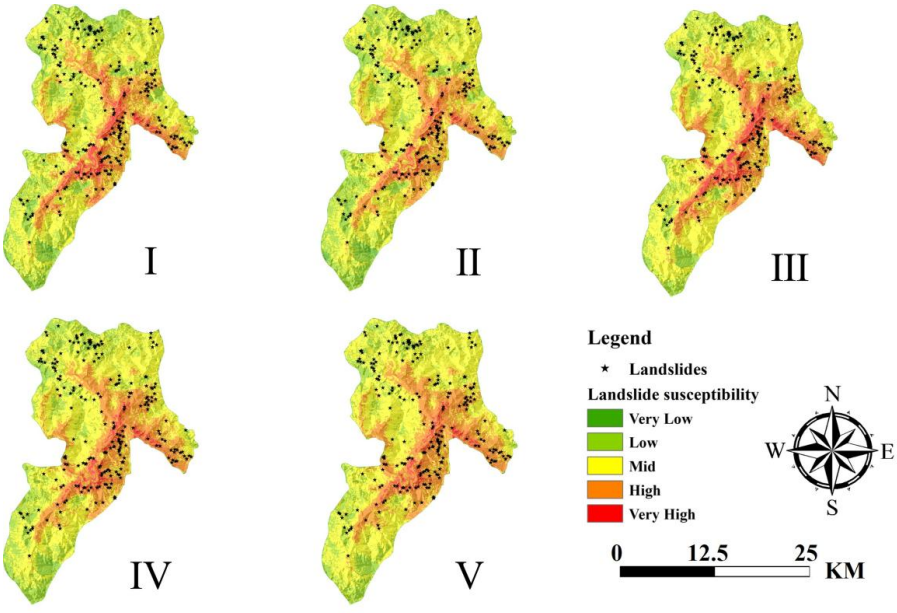

Fig. 10. Landslide Susceptibility Distribution Map for Five Scenarios

When rainfall and vegetation factors are considered together (Category IV), the very low and low susceptibility zones decrease by 33.12 km², while the medium susceptibility zones increase by 18.25 km², with ten fewer landslides. The high susceptibility zone expands by 23.66 km², with 19 additional landslides. Although the very high susceptibility zone shrinks in area, disaster point density increases to 0.61 per km².Adding the wind speed factor (Category V) causes the very low and low

https://doi.org/10.5194/egusphere-2025-3004
Preprint. Discussion started: 9 September 2025

susceptibility zones to decrease significantly by 69.06 km²—almost double the reduction observed in Category IV. The medium and high susceptibility zones expand significantly by 40.25 km² and 38.4 km², respectively. Together, the high and very high susceptibility zones experienced 23 more landslides.

Four patterns emerge: (1) In areas with low NDVI and rainfall, landslide susceptibility shifts from very low to low; (2) In areas with high NDVI and slightly lower rainfall, susceptibility changes from low to medium; (3) In areas with low NDVI and high rainfall, landslide susceptibility shows little change; (4) In areas with high NDVI and rainfall, susceptibility shifts from medium to high.

In summary, vegetation's role in landslide occurrence is influenced by external environmental conditions. This aligns landslide stability models that consider the self-weight of vegetation. It is essential to recognize the double-edged nature of vegetation in landslide prevention and control.

4.3 Mechanisms of landslides in areas with high vegetation coverage

The mechanisms of landslide occurrence in areas with high vegetation coverage represent an important yet underexplored topic. Good vegetation coverage can create a false sense of safety and stability. First, Dense vegetation can obscure surface changes, making it difficult to detect geological or erosion, leading to an underestimation of risks. Secondly, while vegetation coverage can slow down rainwater flow and reduce its impact during initial stages or under conditions of low rainfall over a short period, the dense root networks increase soil stability, thereby enhancing the soil's resistance to landslide initiation. However, areas with good vegetation coverage are often regions

https://doi.org/10.5194/egusphere-2025-3004
Preprint. Discussion started: 9 September 2025

with favorable water and thermal conditions. Vegetation's absorption of part of the rainfall also increases soil saturation, further exacerbating the risks of landslides and debris flows. Under persistent warm and humid conditions, geological and surface changes in high vegetation areas are often gradual. Signs of disasters may accumulate over long timescales, making these changes easy to overlook. Moreover, factors such as seasonal rainfall or snowmelt can increase disaster risks during specific periods, while other times may seem relatively safe. This seasonal variability adds uncertainty to disaster occurrences, further enhancing their concealed nature.

Furthermore, terrain complexity is a key factor contributing to the concealed nature of landslides in areas with high vegetation. These regions often feature rugged terrain with significant elevation changes, which may hide numerous geological structural issues. Such structures can lead to landslides under certain conditions, but their prediction is challenging due to the terrain's complexity. For instance, localized soil erosion or slope collapses might occur in these terrains, but the vegetation cover can make such signs difficult to observe.

Where terrain and rainfall factors combine, vegetation can amplify disaster effects. For instance, strong winds can destabilize vegetated slopes, increasing the risk of soil erosion and landslides. Thus, the concealed mechanisms of landslides result from the combined effects of geological, meteorological, and topographical factors. Comprehensive analysis of these factors is essential to understand hidden risks. Strengthening early warning systems and implementing preventive measures are critical to reducing potential casualties and property losses.

https://doi.org/10.5194/egusphere-2025-3004
Preprint. Discussion started: 9 September 2025

4.4 Comparison with previous studies and scope for future research

Cui et al. (2024) analyzed the characteristics and causes of a similar landslide in this area using Massflow V2.8 simulations. They identified rainfall and human activities as key triggers, but insufficiently addressed interactions between soil, moisture, and external forces (such as natural wind and human mining activities) under high vegetation conditions. This limited simulation accuracy.

The current study uses macroscopic susceptibility mapping to elucidate the interaction mechanisms among landslide susceptibility factors, with vegetation as the core medium. Microscopic stress analysis of slope stability was used to calculate slope stability while accounting for vegetation self-weight. The findings provide an important reference for studying landslide movement characteristics and developing disaster prevention and mitigation strategies in high vegetation mountainous areas.

Although this study analyzes landslides at the watershed scale and specific points. further research is needed at regional, national and global scales to understand the factors influencing both the positive and negative roles of vegetation in landslide prevention. In particular, the specific causes, damage patterns, and impacts of the negative effects remain unclear. On the basis of clarifying the interactions between vegetation and environmental factors (such as rainfall, slope gradient, lithology, and soil thickness), efforts should be made to construct regional or global zoning maps of dominant factors for mountain hazards, considering vegetation and its synergistic factors.

Additionally, while each of the conventional approaches to landslide susceptibility

https://doi.org/10.5194/egusphere-2025-3004
Preprint. Discussion started: 9 September 2025

assessment—such as the information value method, deterministic coefficient method, and analytic hierarchy process (AHP)—have advantages, they also have drawbacks, including high subjectivity, limited explanatory power, and limited applicability. It is challenging to fulfill the present standards for high-precision and high-efficiency landslide risk assessments because of these limitations. Machine learning technologies, have been widely applied in landslide susceptibility assessments. LightGBM and XGBoost have shown excellent performance in susceptibility assessments, but lack interpretability, limiting their credibility. Advances in interpretable machine learning could integrate agent-based models to simulate spatial interactions of factors. Combining these with tools such as GeoDetector and SEM would provide data and form the foundation for developing effective landslide prevention strategies.

5 Conclusion

This study integrates regional landslide susceptibility mapping with stability analysis of typical landslides, revealing spatial variation patterns and mechanisms of landslide susceptibility in high vegetation areas. It clarifies the positive and negative roles of vegetation in landslide prevention and control. While offering insights into the role of vegetation in ecological disaster reduction, the landslide mapping in this study relies on traditional methods. Although these methods have little impact on the overall distribution patterns of landslide susceptibility, they exhibit limited precision to some extent, particularly in small watersheds, where the evaluation results are coarse. With the continuous advancement of machine learning techniques, leveraging these methods' interpretability and strong learning capabilities can further improve the accuracy of

https://doi.org/10.5194/egusphere-2025-3004
Preprint. Discussion started: 9 September 2025

landslide susceptibility mapping in future studies. This study gives limited consideration to factors such as earthquakes, forest height, and root distribution. By incorporating more extensive datasets in future research, the changes in landslide susceptibility and its driving forces can be better understood. In summary, this study examines the role of vegetation in landslides from both macro and micro perspectives, providing theoretical support for further landslide risk assessments.

Code and data availability

Data will be made available on request. Please contact the first author regarding the availability of code and data used in this work.

Author contributions

Songtang He: writing – original draft, visualization, validation, data curation. **Zhenhong Shen and Yuqing Yang:** software, methodology, formal analysis. **Jeffrey Neal, Xudong Hu, and Yongming Lin:** writing – review & editing. **Zongji Yang, Jiangang Chen, Daojie Wang:** investigation, supervision, resources. **Youtong Rong, Yanchen Zheng, Xiaoli Su, and Yong Kong:** review & editing, data check, validation.

Competing interests

The contact author has declared that none of the authors has any competing interests.

Acknowledgements

This work was financially supported by the National Key R&D Program of China (2024YFC3012702; 2024YFF1307801; 2024YFF1307800), the Youth Innovation Promotion Association of the Chinese Academy of Sciences (Grant No. 2023389), the National Natural Science Foundation of China (Grant No. 42201094; Grant No.

https://doi.org/10.5194/egusphere-2025-3004
Preprint. Discussion started: 9 September 2025

42371014), the Science and Technology Research Program of the Institute of Mountain Hazards and Environment, Chinese Academy of Sciences (Grant No. IMHE-CXTD-01), China Scholarship Council (CSC) for Academic Visiting (202404910203).

Declaration of interest Statement

The authors declare that they have no known competing financial interests or personal relationships that could have appeared to influence the work reported in this paper.

References

Ahmad, M. S., MonaLisa, & Khan, S. (2023). Comparative analysis of analytical hierarchy process (AHP) and frequency ratio (FR) models for landslide susceptibility mapping in Reshun, NW Pakistan. *Kuwait Journal of Science*, 50(3), 387-398. https://doi.org/10.1016/j.kjs.2023.01.004

Alvioli, M., Loche, M., Jacobs, L., Grohmann, C. H., Abraham, M. T., Gupta, K., Satyam, N., Scaringi, G., Bornaetxea, T., Rossi, M., Marchesini, I., Lombardo, L., Moreno, M., Steger, S., Camera, C. A. S., Bajni, G., Samodra, G., Wahyudi, E. E., Susyanto, N., Sinčić, M., Gazibara, S. B., Sirbu, F., Torizin, J., Schüßler, N., Mirus, B. B., Woodard, J. B., Aguilera, H., & Rivera-Rivera, J. (2024). A benchmark dataset and workflow for landslide susceptibility zonation. *Earth-Science Reviews*, 258, 104927. https://doi.org/10.1016/j.earscirev.2024.104927

Arabameri, A., Pradhan, B., Rezaei, K., Sohrabi, M., & Kalantari, Z. (2019). GIS-based landslide susceptibility mapping using numerical risk factor bivariate model and its ensemble with linear multivariate regression and boosted regression tree algorithms. *Journal of Mountain Science*, 16(3), 595-618. http://doi.org/10.1007/s11629-018-5168-y

Asmare, D. (2023). Application and validation of AHP and FR methods for landslide susceptibility mapping around choke mountain, northwestern ethiopia. *Scientific African*, 19, e1470. http://doi.org/https://doi.org/10.1016/j.sciaf.2022.e01470

Bordoloi, S., & Ng, C. W. W. (2020). The effects of vegetation traits and their stability functions in bio-engineered slopes: A perspective review. *Engineering Geology*, 275, 105742. https://doi.org/10.1016/j.enggeo.2020.105742

Chen, C., Liu, Y., Li, Y., & Guo, F. (2024). Mapping landslide susceptibility with the consideration of spatial heterogeneity and factor optimization. *Natural Hazards* http://doi.org/10.1007/s11069-024-06955-w

Chen, W., Li, H., Hou, E., Wang, S., Wang, G., Panahi, M., Li, T., Peng, T., Guo, C., Niu, C., Xiao, L., Wang, J., Xie, X., & Ahmad, B. B. (2018). GIS-based groundwater potential analysis using novel ensemble weights-of-evidence with logistic regression and functional tree models. *Science of the Total Environment*,

https://doi.org/10.5194/egusphere-2025-3004
Preprint. Discussion started: 9 September 2025

634, 853-867. https://doi.org/10.1016/j.scitotenv.2018.04.055

Chicas, S. D., Li, H., Mizoue, N., Ota, T., Du, Y., & Somogyvári, M. (2024). Landslide susceptibility mapping core-base factors and models' performance variability: a systematic review. *Natural Hazards*, 120(14), 12573-12593. http://doi.org/10.1007/s11069-024-06697-9

Cui, Y., Qian, Z., Xu, W., & Xu, C. (2024). A Small-Scale Landslide in 2023, Leshan, China: Basic Characteristics, Kinematic Process and Cause Analysis. *Remote Sensing*, 16(17), 3324. http://doi.org/10.3390/rs16173324

Deng, J., Ma, C., & Zhang, Y. (2022). Shallow landslide characteristics and its response to vegetation by example of July 2013, extreme rainstorm, Central Loess Plateau, China. *Bulletin of Engineering Geology and the Environment*, 81(3), 100. http://doi.org/10.1007/s10064-022-02606-1

Dhanai, P., Singh, V.P. & Soni, P. Rainfall Triggered Slope Instability Analysis with Changing Climate. *Indian Geotech J* **52**, 477–492 (2022). https://doi.org/10.1007/s40098-021-00581-0

Fan, Y., Chen, J., Shirkey, G., John, R., Wu, S. R., Park, H., & Shao, C. (2016). Applications of structural equation modeling (SEM) in ecological studies: an updated review. *Ecological Processes*, 5(1), 19. http://doi.org/10.1186/s13717-016-0063-3

Gonzalez-Ollauri, A., & Mickovski, S. B. (2016). Using the root spread information of pioneer plants to quantify their mitigation potential against shallow landslides and erosion in temperate humid climates. *Ecological Engineering*, 95, 302-315. https://doi.org/10.1016/j.ecoleng.2016.06.028

Goren, L., Aharonov, E., & Anders, M. H. (2010). The long runout of the Heart Mountain landslide: Heating, pressurization, and carbonate decomposition. *Journal of Geophysical Research: Solid Earth*, 115(B10) http://doi.org/10.1029/2009JB007113

He, S., Wang, D., Fang, Y., & Lan, H. (2017). Guidelines for integrating ecological and biological engineering technologies for control of severe erosion in mountainous areas – A case study of the Xiaojiang River Basin, China. *International Soil and Water Conservation Research*, 5(4), 335-344. https://doi.org/10.1016/j.iswcr.2017.05.001

He, S., Yang, H., Chen, X., Wang, D., Lin, Y., Pei, Z., Li, Y., & Akbar Jamali, A. (2024). Ecosystem sensitivity and landscape vulnerability of debris flow waste-shoal land under development and utilization changes. *Ecological Indicators*, 158, 111335. https://doi.org/10.1016/j.ecolind.2023.111335

Hengl, T., Mendes De Jesus, J., Heuvelink, G. B. M., Ruiperez Gonzalez, M., Kilibarda, M., Blagotić, A., Shangguan, W., Wright, M. N., Geng, X., Bauer-Marschallinger, B., Guevara, M. A., Vargas, R., MacMillan, R. A., Batjes, N. H., Leenaars, J. G. B., Ribeiro, E., Wheeler, I., Mantel, S., & Kempen, B. (2017). SoilGrids250m: Global gridded soil information based on machine learning. *Plos One*, 12(2), e169748. https://doi.org/10.1371/journal.pone.0169748

Hu, L. T., & Bentler, P. M. (1999). Cutoff criteria for fit indexes in covariance structure analysis: Conventional criteria versus new alternatives. *Structural Equation*

https://doi.org/10.5194/egusphere-2025-3004
Preprint. Discussion started: 9 September 2025

Modeling: A Multidisciplinary Journal, 6(1), 1-55. http://doi.org/10.1080/10705519909540118

Khosravi, K., Shahabi, H., Pham, B. T., Adamowski, J., Shirzadi, A., Pradhan, B., Dou, J., Ly, H., Gróf, G., & Ho, H. L. (2019). A comparative assessment of flood susceptibility modeling using multi-criteria decision-making analysis and machine learning methods. *Journal of Hydrology*, 573, 311-323. https://doi.org/10.1016/j.jhydrol.2019.03.073

Lan, H., Wang, D., He, S., Fang, Y., Chen, W., Zhao, P., & Qi, Y. (2020). Experimental study on the effects of tree planting on slope stability. *Landslides*, 17(4), 1021-1035. http://doi.org/10.1007/s10346-020-01348-z

Li, Z., Guo, J., Li, T. *et al.* Influence of topography on the fragmentation and mobility of landslides. *Bull Eng Geol Environ* **84**, 73 (2025). https://doi.org/10.1007/s10064-025-04095-4

Liu, W., Yang, Z., & He, S. (2020). Modeling the landslide-generated debris flow from formation to propagation and run-out by considering the effect of vegetation. *Landslides*, 18, 43-58. https://doi.org/10.1007/s10346-020-01478-4

Liu, X., Shao, S., & Shao, S. (2024). Landslide susceptibility zonation using the analytical hierarchy process (AHP) in the Great Xi'an Region, China. *Scientific Reports*, 14(1), 2941. http://doi.org/10.1038/s41598-024-53630-y

Lu, F., Zhang, G., Wang, T., Ye, Y., Zhen, J., & Tu, W. (2024). Analyzing spatial non-stationarity effects of driving factors on landslides: a multiscale geographically weighted regression approach based on slope units. *Bulletin of Engineering Geology and the Environment*, 83(10), 394. http://doi.org/10.1007/s10064-024-03879-4

Manzella, I., Labiouse, V., & Barla, G. (2008). Qualitative analysis of rock avalanches propagation by means of physical modelling of non-constrained gravel flows. *Rock Mechanics and Rock Engineering*, 41(1), 133-151. http://doi.org/10.1007/s00603-007-0134-y

Medina, V., Hürlimann, M., Guo, Z., Lloret, A., & Vaunat, J. (2021). Fast physically-based model for rainfall-induced landslide susceptibility assessment at regional scale. *Catena*, 201, 105213. https://doi.org/10.1016/j.catena.2021.105213

Murgia, I., Giadrossich, F., Mao, Z., Cohen, D., Capra, G. F., & Schwarz, M. (2022). Modeling shallow landslides and root reinforcement: A review. *Ecological Engineering*, 181, 106671. https://doi.org/10.1016/j.ecoleng.2022.106671

Ng, C. W. W., Yang, B., Liu, Z. Q., Kwan, J. S. H., & Chen, L. (2021). Spatiotemporal modelling of rainfall-induced landslides using machine learning. *Landslides*, 18(7), 2499-2514. http://doi.org/10.1007/s10346-021-01662-0

Oberhänsli, R., Ogawa, Y., & Komac, M. (2017). *International Union of Geological Sciences (IUGS)—Sendai—Foreseeable but Unpredictable Geologic Events—IUGS Reactions*. Paper presented at the, Cham.

Ortiz-Giraldo L, Botero BA and Vega J (2023) An integral assessment of landslide dams generated by the occurrence of rainfall-induced landslide and debris flow hazard chain. *Front. Earth Sci.* 11:1157881. http://doi.org/10.3389/feart.2023.1157881

Peng, S. (2020). 1-km monthly precipitation dataset for China (1901-2023). National

https://doi.org/10.5194/egusphere-2025-3004
Preprint. Discussion started: 9 September 2025

Tibetan Plateau / Third Pole Environment Data Center. https://doi.org/10.5281/zenodo.3114194.

Pokharel, B., Althuwaynee, O. F., Aydda, A., Kim, S., Lim, S., & Park, H. (2021). Spatial clustering and modelling for landslide susceptibility mapping in the north of the Kathmandu Valley, Nepal. *Landslides*, 18(4), 1403-1419. http://doi.org/10.1007/s10346-020-01558-5

Pourghasemi, H. R., Teimoori Yansari, Z., Panagos, P., & Pradhan, B. (2018). Analysis and evaluation of landslide susceptibility: a review on articles published during 2005–2016 (periods of 2005–2012 and 2013–2016). *Arabian Journal of Geosciences*, 11(9), 193. http://doi.org/10.1007/s12517-018-3531-5

Qin, M., Cui, P., Jiang, Y. et al. Occurrence of shallow landslides triggered by increased hydraulic conductivity due to tree roots. Landslides 19, 2593–2604 (2022). https://doi.org/10.1007/s10346-022-01921-8

Regmi, N. R., Giardino, J. R., & Vitek, J. D. (2010). Modeling susceptibility to landslides using the weight of evidence approach; western Colorado, USA. *Geomorphology (Amsterdam, Netherlands)*, 115(1-2), 172-187. http://doi.org/10.1016/j.geomorph.2009.10.002

Rey, F., Bifulco, C., Bischetti, G. B., Bourrier, F., De Cesare, G., Florineth, F., Graf, F., Marden, M., Mickovski, S. B., Phillips, C., Peklo, K., Poesen, J., Polster, D., Preti, F., Rauch, H. P., Raymond, P., Sangalli, P., Tardio, G., & Stokes, A. (2019). Soil and water bioengineering: Practice and research needs for reconciling natural hazard control and ecological restoration. *Science of the Total Environment*, 648, 1210-1218. http://doi.org/https://doi.org/10.1016/j.scitotenv.2018.08.217

Roback, K., Clark, M. K., West, A. J., Zekkos, D., Li, G., Gallen, S. F., Chamlagain, D., & Godt, J. W. (2018). The size, distribution, and mobility of landslides caused by the 2015 Mw7.8 Gorkha earthquake, Nepal. *Geomorphology*, 301, 121-138. http://doi.org/10.1016/j.geomorph.2017.01.030

Schmaltz, E. M., & Mergili, M. (2018). Integration of root systems into a GIS-based slip surface model: computational experiments in a generic hillslope environment. *Landslides*, 15(8), 1561-1575. http://doi.org/10.1007/s10346-018-0970-8

Segoni, S., Ajin, R. S., Nocentini, N., & Fanti, R. (2024). Insights Gained from the Review of Landslide Susceptibility Assessment Studies in Italy. *Remote Sensing*, *16*(23), 4491. https://doi.org/10.3390/rs16234491

Sezer, E. A., Pradhan, B., & Gokceoglu, C. (2010). Manifestation of an adaptive neuro-fuzzy model on landslide susceptibility mapping: Klang valley, Malaysia. *Expert Systems with Applications*, 38(7), 8208-8219. http://doi.org/10.1016/j.eswa.2010.12.167

Stone, B. M. (2021). The Ethical Use of Fit Indices in Structural Equation Modeling: Recommendations for Psychologists. *Frontiers in Psychology*, 12

Su, X., Wei, W., Ye, W., Meng, X., & Wu, W. (2019). Predicting landslide sliding distance based on energy dissipation and mass point kinematics. *Natural Hazards*, 96(3), 1367-1385. http://doi.org/10.1007/s11069-019-03618-z

Vergani, C., Giadrossich, F., Buckley, P., Conedera, M., Pividori, M., Salbitano, F., Rauch, H. S., Lovreglio, R., & Schwarz, M. (2017). Root reinforcement dynamics

https://doi.org/10.5194/egusphere-2025-3004
Preprint. Discussion started: 9 September 2025

of European coppice woodlands and their effect on shallow landslides: A review. *Earth-Science Reviews*, 167, 88-102. http://doi.org/https://doi.org/10.1016/j.earscirev.2017.02.002

Wang, J. F., Li, X. H., Christakos, G., Liao, Y. L., Zhang, T., Gu, X., & Zheng, X. Y. (2010). Geographical Detectors-Based Health Risk Assessment and its Application in the Neural Tube Defects Study of the Heshun Region, China. *International Journal of Geographical Information Science*, 24(1), 107-127. http://doi.org/10.1080/13658810802443457

Wang, Y. A., & Rhemtulla, M. (2021). Power Analysis for Parameter Estimation in Structural Equation Modeling: A Discussion and Tutorial. *Advances in Methods and Practices in Psychological Science*, 4(1), 1403230957. http://doi.org/10.1177/2515245920918253

Wang, Y., Feng, L., Li, S., Ren, F., & Du, Q. (2020). A hybrid model considering spatial heterogeneity for landslide susceptibility mapping in Zhejiang Province, China. *Catena*, 188, 104425. http://doi.org/https://doi.org/10.1016/j.catena.2019.104425

Xu, X. (2022a). China 30m Annual Maximum NDVI Dataset: Resource and Environment Science Data Registration and Publishing System. https://doi.org/10.12078/2022030801

Xu, X. (2022b). China Annual Spatial Interpolation Dataset of Meteorological Elements: Resource and Environment Science Data Registration and Publishing System. https://doi.org/10.12078/2022082501

Xu, Y., Luo, L., Guo, W., Jin, Z., Tian, P., & Wang, W. (2024). Revegetation Changes Main Erosion Type on the Gully–Slope on the Chinese Loess Plateau Under Extreme Rainfall: Reducing Gully Erosion and Promoting Shallow Landslides. *Water Resources Research*, 60(3), e2023WR036307. https://doi.org/10.1029/2023WR036307

Yang, L., Ji, X., Li, M., Yang, P., Jiang, W., Chen, L., Yang, C., Sun, C., & Li, Y. (2024). A comprehensive framework for assessing the spatial drivers of flood disasters using an Optimal Parameter-based Geographical Detector–machine learning coupled model. *Geoscience Frontiers*, 15(6), 101889. https://doi.org/10.1016/j.gsf.2024.101889

Yilmaz, I. (2009). Landslide susceptibility mapping using frequency ratio, logistic regression, artificial neural networks and their comparison: A case study from Kat landslides (Tokat—Turkey). *Computers & Geosciences*, 35(6), 1125-1138. http://doi.org/10.1016/j.cageo.2008.08.007

Zhang, Y., Li, y., Tom Dijkstra., Janusz Wasowski., Meng, X., Wu, X., Liu, W., Chen, G. (2025). Evolution of large landslides in tectonically active regions - A decade of observations in the Zhouqu County, China. Engineering Geology, 348, 107967. https://doi.org/10.1016/j.enggeo.2025.107967